

Phenomenological study of two minor zeros in neutrino mass matrix using trimaximal mixing

Iffat Ara Mazumder* and Rupak Dutta†
National Institute of Technology Silchar, Silchar 788010, India

We study the phenomenological implications of two minor zeros in neutrino mass matrix using trimaximal mixing matrix. In this context, we analyse fifteen possible cases of two minor zeros in neutrino mass matrix and found only two cases, namely Class A_1 and Class A_2 , that are compatible with the present neutrino oscillation data. We present correlations of several neutrino oscillation parameters and give prediction of the total neutrino mass, the values of effective Majorana mass, the effective electron anti-neutrino mass and CP violating Majorana phases for these two classes. We also explore the degree of fine tuning in the elements of neutrino mass matrix for the allowed classes. Moreover, we propose a flavor model within the seesaw model along with Z_8 symmetry group that can generate such classes.

PACS numbers: 14.60.Pq, 14.60.St, 23.40.s

I. INTRODUCTION

Although no new particles beyond the Standard Model (SM) have been discovered in any experiments so far, but the neutrino oscillation phenomena observed in several experiments [1, 2] indirectly confirms the existence of a more global theory beyond the SM. The non zero neutrino mass as confirmed by neutrino oscillation experiments can not be explained by the SM and its origin is one of the most fundamental questions in particle physics today. In the flavor basis where the charged lepton mass matrix is diagonal, the neutrino mass matrix M can be parametrized in terms of nine free parameters, namely three masses (m_1, m_2, m_3), three mixing angles ($\theta_{12}, \theta_{13}, \theta_{23}$), two Majorana CP violating phases (α, β) and a Dirac CP violating phase (δ). Although the mixing angles and the mass squared differences are known to a very good accuracy from currently available experimental data, there are still many open questions in the neutrino sector. For instance, the absolute mass scale of three neutrinos, the sign of Δm_{32}^2 , whether neutrinos are Dirac or Majorana particle, the three CP violating phases are still unknown. With the experimental values of the mass squared differences and the mixing angles as the input parameters, we still have four unknown parameters in the neutrino mass matrix M . There exists several schemes in literature by which one can reduce the number of free parameters in the neutrino mass matrix. The general idea is to assume that some matrix elements will be dependent on other matrix elements. For instance, one can assume certain matrix element to be zero or certain combination of elements of the neutrino mass matrix to be zero that can be caused by some underlying flavor symmetry.

The exact mechanism of the origin of neutrino masses is still unknown. Out of many proposed theoretical models, the seesaw mechanism of either type-I or type-II looks more promising. The seesaw mechanism not only helps in understanding the scale of neutrino mass but also provide the necessary ingredients to realize texture zero patterns in the neutrino mass matrix. Within the framework of Type-I seesaw mechanism [3, 4], the neutrino mass matrix is written as

$$M = -M_D M_R^{-1} M_D^T, \quad (1)$$

where M_D is the 3×3 Dirac mass matrix that links $(\nu_e, \nu_\mu, \nu_\tau)$ to their right handed singlet counterpart and M_R is the 3×3 Majorana mass matrix of the right handed neutrinos. It is worth mentioning that by considering the suitable position of zeros in M_D and M_R , one can, in principle, get the desired zero textures of the neutrino mass matrix. It should also be noted that zeros in M_D and M_R not only give rise to zeros in the mass matrix but also give rise to zero minors in the neutrino mass matrix. It was also pointed out in Ref. [5, 6] that if M_D is diagonal, then zeros in M_R can give rise to minor zero pattern in the neutrino mass matrix M .

There exists numerous literatures where the form and texture of the neutrino mass matrix have been explored. It was found that texture with more than two zeros in the neutrino mass matrix can not accommodate the latest neutrino

*Electronic address: iffat_rs@phy.nits.ac.in

†Electronic address: rupak@phy.nits.ac.in

oscillation data. The phenomenology of two texture zeros [7–19] have been explored at large scale in the literature with Pontecorvo Maki Nakagawa Sakata (PMNS) and trimaximal (TM) mixing matrix. It should be noted that out of fifteen possible cases of two texture zeros only seven patterns are favored by the recent experimental data. [7] in case of PMNS mixing matrix. With TM mixing matrix, however, only two patterns are found to be compatible with the oscillation data. [8, 17]. In Ref. [10], the authors investigated viable textures with two zeros in the inverted neutrino mass matrix and seven such patterns were shown to be allowed. However, these textures do not apply in the case of non-invertible neutrino mass matrix M . Also, in Ref. [20, 21], authors have studied the phenomenological implications of one texture zero in neutrino mass matrix and found all six possible patterns to be compatible with the data. Moreover, in Ref. [5, 6, 22–25] and Ref. [26–31] the authors have explored the phenomenology of vanishing minor and cofactor zero in the neutrino mass matrix. The class of one and two independent zero minors textures in the neutrino mass matrix were explored in Refs. [5, 22] with PMNS mixing matrix. It was shown that out of fifteen possible two minor zero patterns, only seven patterns are viable and all the six one minor zero patterns are compatible with the data. Similarly, for TM mixing matrix along with one minor zero condition [6], all the six possible patterns are found to be allowed. In Ref. [24], the authors have used the tribimaximal (TB) mixing matrix and showed that five classes of texture zeros or vanishing minor can accommodate the neutrino oscillation data.

Although TB mixing pattern was studied extensively in literature, it, however, was ruled out due to a non zero value of the reactor mixing angle θ_{13} confirmed by several experiments such as T2K [32], MINOS [33], Double Chooz [34] and Daya Bay [35]. In order to accommodate a non zero value of θ_{13} , TM mixing matrix was constructed by multiplying the TB mixing matrix by an unitary matrix [36–38]. If the first column of the TM mixing matrix is identical to the first column of TB mixing matrix, it is called TM_1 mixing matrix and if the second column is identical to that of the TB mixing matrix it is called TM_2 mixing matrix. In this paper we analyze the compatibility of two minor zero neutrino Majorana textures with the recent experimental data using TM_1 and TM_2 mixing matrix. By using two minor zero conditions one can reduce the number of free parameters in the model. We analyse fifteen possible cases of two minor zeros in neutrino mass matrix and found only two cases, namely class A_1 and class A_2 , that are compatible with the present neutrino oscillation data. In order to study the detail feature of the mass matrix elements we first perform a χ^2 analysis of the allowed two minor zero textures. We use five observables in our χ^2 analysis, namely three mixing angles and the two mass squared differences. We do not use Dirac CP violating phase δ in our χ^2 analysis as its value has not been measured yet. We also find the degree of fine tuning in the neutrino mass matrix elements for each allowed textures. Moreover, We give our model predictions of the unknown Dirac and Majorana CP violating phases, the total neutrino mass, effective Majorana mass and the effective electron anti-neutrino mass for these two classes.

We organize the paper as follows. We start with TM_1 and TM_2 mixing matrix and find the elements of the neutrino mass matrix in Section. II. We then write down θ_{13} , θ_{23} , θ_{12} , Dirac CP violating phase δ , effective electron anti-neutrino mass m_ν and the effective Majorana mass term M_{ee} in terms of the unknown parameters θ and ϕ of the TM mixing matrix. In Section. III, we describe the formalism of two minor zeros in neutrino mass matrix and identify all the possible cases of two minor zero in neutrino mass matrix. In Section. IV, we discuss the phenomenology of the allowed two minor zero classes and obtain the best fit values of all the oscillation parameters with our χ^2 analysis. Also we report the degree of fine-tuning in the neutrino mass matrix elements. In Section. V, we present the symmetry realization of our model and conclude in Section. VI.

II. NEUTRINO MASS MATRIX

TM_1 and TM_2 mixing matrix, constructed by multiplying the TB mixing matrix by an unitary matrix, can be written as

$$U_{TM_1} = \begin{pmatrix} \sqrt{\frac{2}{3}} & \frac{1}{\sqrt{3}} \cos \theta & \frac{1}{\sqrt{3}} \sin \theta \\ -\frac{1}{\sqrt{6}} & \frac{\cos \theta}{\sqrt{3}} - \frac{e^{i\phi} \sin \theta}{\sqrt{2}} & \frac{\sin \theta}{\sqrt{3}} + \frac{e^{i\phi} \cos \theta}{\sqrt{2}} \\ -\frac{1}{\sqrt{6}} & \frac{\cos \theta}{\sqrt{3}} + \frac{e^{i\phi} \sin \theta}{\sqrt{2}} & \frac{\sin \theta}{\sqrt{3}} - \frac{e^{i\phi} \cos \theta}{\sqrt{2}} \end{pmatrix}. \quad (2)$$

and

$$U_{TM_2} = \begin{pmatrix} \sqrt{\frac{2}{3}} \cos \theta & \frac{1}{\sqrt{3}} & \sqrt{\frac{2}{3}} \sin \theta \\ -\frac{\cos \theta}{\sqrt{6}} + \frac{e^{-i\phi} \sin \theta}{\sqrt{2}} & \frac{1}{\sqrt{3}} & -\frac{\sin \theta}{\sqrt{6}} - \frac{e^{-i\phi} \cos \theta}{\sqrt{2}} \\ -\frac{\cos \theta}{\sqrt{6}} - \frac{e^{-i\phi} \sin \theta}{\sqrt{2}} & \frac{1}{\sqrt{3}} & -\frac{\sin \theta}{\sqrt{6}} + \frac{e^{-i\phi} \cos \theta}{\sqrt{2}} \end{pmatrix}. \quad (3)$$

where θ and ϕ are two free parameters. In the flavor basis where the charged lepton mass matrix is diagonal, the symmetric neutrino mass matrix M can be expressed as

$$(M)_{\rho\sigma} = (V M_{diag} V^T)_{\rho\sigma} \text{ with } \rho, \sigma = e, \mu, \tau, \quad (4)$$

where $M_{diag} = \text{diag}(m_1, m_2, m_3)$ is the diagonal matrix containing three mass states. The lepton flavor mixing matrix V can be expressed as $V = U_{TM} P$, where the diagonal phase matrix P can be written as

$$P = \begin{pmatrix} 1 & 0 & 0 \\ 0 & e^{i\alpha} & 0 \\ 0 & 0 & e^{i\beta} \end{pmatrix} \quad (5)$$

that contains two CP violating Majorana phases α and β . For completeness, we report all the elements of the neutrino mass matrix for the TM_1 and TM_2 mixing matrix in Eq. A1 and Eq. A2 of appendix A.

We can express the neutrino oscillation parameters such as the three mixing angles θ_{12} , θ_{23} , θ_{13} , the Jarlskog invariant J [39] and the Dirac CP violating phase δ in terms of the two unknown parameters θ and ϕ of the trimaximal mixing matrix. For TM_1 mixing matrix, we have

$$\begin{aligned} s_{12}^2 &= \frac{|(U_{12})_{TM_1}|^2}{1 - |(U_{13})_{TM_1}|^2} = 1 - \frac{2}{3 - \sin^2 \theta}, \\ s_{23}^2 &= \frac{|(U_{23})_{TM_1}|^2}{1 - |(U_{13})_{TM_1}|^2} = \frac{1}{2} \left(1 + \frac{\sqrt{6} \sin 2\theta \cos \phi}{3 - \sin^2 \theta} \right), \\ s_{13}^2 &= |(U_{13})_{TM_1}|^2 = \frac{1}{3} \sin^2 \theta, \\ J &= \frac{1}{6\sqrt{6}} \sin 2\theta \sin \phi, \\ \csc^2 \delta &= \csc^2 \phi - \frac{6 \sin^2 2\theta \cot^2 \phi}{(3 - \sin^2 \theta)^2} \end{aligned} \quad (6)$$

and for TM_2 mixing matrix, we have

$$\begin{aligned} s_{12}^2 &= \frac{|(U_{12})_{TM_2}|^2}{1 - |(U_{13})_{TM_2}|^2} = \frac{1}{3 - 2 \sin^2 \theta}, \\ s_{23}^2 &= \frac{|(U_{23})_{TM_2}|^2}{1 - |(U_{13})_{TM_2}|^2} = \frac{1}{2} \left(1 + \frac{\sqrt{3} \sin 2\theta \cos \phi}{3 - 2 \sin^2 \theta} \right), \\ s_{13}^2 &= |(U_{13})_{TM_2}|^2 = \frac{2}{3} \sin^2 \theta, \\ J &= \frac{1}{6\sqrt{3}} \sin 2\theta \sin \phi, \\ \csc^2 \delta &= \csc^2 \phi - \frac{3 \sin^2 2\theta \cot^2 \phi}{(3 - 2 \sin^2 \theta)^2}, \end{aligned} \quad (7)$$

where $s_{ij} = \sin \theta_{ij}$ and $c_{ij} = \cos \theta_{ij}$ for $i, j = 1, 2, 3$.

There are several experiments that can, in principle, put constraints on the neutrino mass scale. The β decay experiment performed at Karlsruhe Tritium Neutrino (KATRIN) experiment can measure the effective electron anti-neutrino mass by studying the endpoint region of the β decay spectrum. The current upper bound of the effective electron anti-neutrino mass is reported to be $m_\nu < 0.8$ eV at 90% confidence level [40]. In future KATRIN is expected to reach the mass sensitivity up to 0.2 eV. The next generation β decay experiment such as Project 8 experiment [41] is designed to reach the mass sensitivity up to 0.04 eV. Similarly, the effective Majorana mass term $|M_{ee}|$ can be obtained from the neutrinoless double beta decay experiment. The current upper bound on the value of M_{ee} reported by GERDA experiment obtained by using ^{48}Ca isotope is $M_{ee} < (0.079 - 0.18)$ eV [42]. The KamLAND-Zen and EXO-200 experiments [43, 44] on ^{136}Xe isotope reported the upper limit on M_{ee} to be $M_{ee} < (0.061 - 0.165)$ eV and $M_{ee} < (0.09 - 0.29)$ eV, respectively. It is expected that the next generation experiments can reach the mass sensitivity upto (5 – 20) meV. There are also several results related to the total neutrino mass coming from various cosmological observations. The Planck satellite reported the upper limit on the total neutrino mass combining BAO

data with CMB data to be $\sum m_i < 0.12$ eV at 95% confidence level [45]. The stringent limit on the absolute neutrino mass is obtained by combining CMB lensing and galaxy clustering data and it is found to be $\sum m_i < 0.09$ eV [46].

We can write the effective Majorana mass $|M_{ee}|$ and effective electron anti-neutrino mass m_ν for the TM₁ mixing matrix as

$$|M_{ee}| = \left| \frac{1}{3}(2m_1 + m_2 \cos^2 \theta e^{2i\alpha} + m_3 \sin^2 \theta e^{2i\beta}) \right|. \quad (8)$$

$$m_\nu^2 = \sum_{i=1}^3 m_i^2 U_{ie}^2 = \frac{1}{3}(2m_1^2 + m_2^2 \cos^2 \theta + m_3^2 \sin^2 \theta). \quad (9)$$

For TM₂ mixing matrix, $|M_{ee}|$ and m_ν can be expressed as

$$|M_{ee}| = \left| \frac{1}{3}(2m_1 \cos^2 \theta + m_2 e^{2i\alpha} + 2m_3 \sin^2 \theta e^{2i\beta}) \right|. \quad (10)$$

$$m_\nu^2 = \frac{1}{3}(2m_1^2 \cos^2 \theta + m_2^2 + 2m_3^2 \sin^2 \theta). \quad (11)$$

The most stringent constraint on any model required to fit the data comes from the ratio of the absolute values of the solar and atmospheric mass squared differences characterized by

$$r \equiv \left| \frac{\Delta m_{21}^2}{\Delta m_{32}^2} \right|, \quad (12)$$

where Δm_{21}^2 and Δm_{32}^2 represent solar and atmospheric mass squared differences, respectively. With the latest experimental values of Δm_{21}^2 and Δm_{32}^2 , one can estimate the value of r to be $(2.95 \pm 0.08) \times 10^{-2}$.

III. TWO MINOR ZEROS IN NEUTRINO MASS MATRIX

The neutrino mass matrix constructed using the trimaximal mixing matrix is a 3×3 symmetric matrix and has six independent entries. Hence we have six independent minors corresponding to each independent entries in the mass matrix. There are total 6C_2 or 15 possible ways to have two minor zeros in the mass matrix. All the fifteen possible patterns of two minor zero in neutrino mass matrix are listed in Table. I. We denote the minor corresponding to ij^{th} element of M_{ij} as C_{ij} .

Class	Constraining equations
A_1	$C_{33} = 0, C_{32} = 0$
A_2	$C_{22} = 0, C_{32} = 0$
B_3	$C_{33} = 0, C_{31} = 0$
B_4	$C_{22} = 0, C_{21} = 0$
B_5	$C_{33} = 0, C_{12} = 0$
B_6	$C_{22} = 0, C_{13} = 0$
D	$C_{33} = 0, C_{22} = 0$
S_1	$C_{31} = 0, C_{11} = 0$
S_2	$C_{21} = 0, C_{11} = 0$
S_3	$C_{13} = 0, C_{12} = 0$
F_1	$C_{33} = 0, C_{11} = 0$
F_2	$C_{22} = 0, C_{11} = 0$
F_3	$C_{32} = 0, C_{11} = 0$
F_4	$C_{31} = 0, C_{32} = 0$
F_5	$C_{21} = 0, C_{32} = 0$

TABLE I: Two minor zero patterns.

In terms of neutrino mass matrix elements, the conditions for two minor zero can be written as

$$\begin{aligned} M_{ab}M_{cd} - M_{uv}M_{wx} &= 0, \\ M_{a'b'}M_{c'd'} - M_{u'v'}M_{w'x'} &= 0. \end{aligned} \quad (13)$$

We can write Eq. 13 in terms of a complex equation as

$$\begin{aligned} m_1 m_2 X_3 e^{2i\alpha} + m_2 m_3 X_1 e^{2i(\alpha+\beta)} + m_3 m_1 X_2 e^{2i\beta} &= 0, \\ m_1 m_2 Y_3 e^{2i\alpha} + m_2 m_3 Y_1 e^{2i(\alpha+\beta)} + m_3 m_1 Y_2 e^{2i\beta} &= 0, \end{aligned} \quad (14)$$

where

$$\begin{aligned} X_k &= (U_{ai} U_{bi} U_{cj} U_{dj} - U_{ui} U_{vi} U_{wj} U_{xj}) + (i \leftrightarrow j), \\ Y_k &= (U_{a'i} U_{b'i} U_{c'j} U_{d'j} - U_{u'i} U_{v'i} U_{w'j} U_{x'j}) + (i \leftrightarrow j), \end{aligned} \quad (15)$$

with (i, j, k) as the cyclic permutation of $(1, 2, 3)$. Using Eq. 14, one can write the mass ratios as

$$\begin{aligned} \frac{m_1}{m_2} e^{-2i\alpha} &= \frac{X_3 Y_1 - X_1 Y_3}{X_2 Y_3 - X_3 Y_2}, \\ \frac{m_1}{m_3} e^{-2i\beta} &= \frac{X_1 Y_2 - X_2 Y_1}{X_2 Y_3 - X_3 Y_2}, \\ \frac{m_3}{m_2} e^{-2i(\alpha-\beta)} &= \frac{X_3 Y_1 - X_1 Y_3}{X_1 Y_2 - X_2 Y_1}. \end{aligned} \quad (16)$$

Similarly, the CP-violating Majorana phases can be written as

$$\begin{aligned} \alpha &= -\frac{1}{2} \arg\left(\frac{X_3 Y_1 - X_1 Y_3}{X_2 Y_3 - X_3 Y_2}\right), \\ \beta &= -\frac{1}{2} \arg\left(\frac{X_1 Y_2 - X_2 Y_1}{X_2 Y_3 - X_3 Y_2}\right). \end{aligned} \quad (17)$$

The value of m_1 , m_2 and m_3 can be calculated using Eq. 16 and mass square differences Δm_{21}^2 and Δm_{32}^2 . That is

$$\begin{aligned} m_1 &= \sqrt{\Delta m_{21}^2} \sqrt{\frac{|\frac{m_1}{m_2}|^2}{|1 - |\frac{m_1}{m_2}|^2|}}, \\ m_2 &= \sqrt{|\Delta m_{32}^2|} \sqrt{\frac{1}{\left||\frac{m_3}{m_2}|^2 - 1\right|}}, \\ m_3 &= \sqrt{|\Delta m_{32}^2|} \sqrt{\frac{1}{|1 - |\frac{m_2}{m_3}|^2|}}. \end{aligned} \quad (18)$$

We can now explore whether or not the chosen texture of the neutrino mass matrix is empirically acceptable. We can construct the mass matrix by using the allowed values of the experimental input parameters such as the mixing angles, mass squared differences and ratio r and test whether or not the other experimental constraints are respected. We now proceed to discuss our results.

IV. RESULTS AND DISCUSSION

Our main aim is to study the phenomenological implication of two minor zeros in the neutrino mass matrix on the total neutrino mass, the effective Majorana mass term, the electron anti-neutrino mass and Majorana CP violating phases. From Eq. 17, it is clear that the CP violating Majorana phases α and β depend on θ and ϕ . Similarly, from Eq. 18, it is clear that neutrino mass m_i depends not only on θ , ϕ but also on the mass squared differences Δm_{21}^2 and Δm_{32}^2 . Moreover, all the neutrino oscillation parameters also depend only on the value of θ and ϕ . We first perform a χ^2 analysis to find the best fit values of our model parameters θ and ϕ and test the validity of our model. We define the χ^2 as follows:

$$\chi^2 = \sum_{i=1}^3 \frac{(\theta_i^{cal} - \theta_i^{exp})^2}{(\sigma_i^{exp})^2} + \sum_{j=21,32} \frac{(\Delta m_j^{cal} - \Delta m_j^{exp})^2}{(\sigma_j^{exp})^2}, \quad (19)$$

where $\theta_i = (\theta_{12}, \theta_{13}, \theta_{23})$ and $\Delta m_j = (\Delta m_{21}^2, \Delta m_{32}^2)$. Here θ_i^{cal} and Δm_j^{cal} represent the calculated value of θ_i and Δm_j , respectively, whereas, θ_i^{exp} and Δm_j^{exp} are the measured central values of θ_i and Δm_j , respectively. The θ_i^{cal}

and Δm_j^{cal} depend on two unknown model parameters, namely θ and ϕ . The σ_i^{exp} and σ_j^{exp} are the uncertainties corresponding to the measured value of θ_i and Δm_j respectively. The central values and the corresponding uncertainties in each parameter, obtained from NuFIT [47], are reported in Table. II. Besides the best fit values of θ and ϕ , the χ^2 analysis also will return the best fit values of the neutrino oscillation parameters such as the three mixing angles and the two mass squared differences for each class of two minor zero patterns. Moreover, we use the 3σ allowed range of r to check the validity of our model.

parameter	Normal ordering(best fit)		inverted ordering ($\Delta\chi^2 = 7.1$)	
	bf $\pm 1\sigma$	3σ ranges	bf $\pm 1\sigma$	3σ ranges
θ_{12}°	$33.44^{+0.77}_{-0.74}$	31.27 \rightarrow 35.86	$33.45^{+0.77}_{-0.74}$	31.27 \rightarrow 35.87
θ_{23}°	$49.2^{+1.0}_{-1.3}$	39.5 \rightarrow 52.0	$49.5^{+1.0}_{-1.2}$	39.8 \rightarrow 52.1
θ_{13}°	$8.57^{+0.13}_{-0.12}$	8.20 \rightarrow 8.97	$8.60^{+0.12}_{-0.12}$	8.24 \rightarrow 8.98
δ°	194^{+52}_{-25}	105 \rightarrow 405	287^{+27}_{-32}	192 \rightarrow 361
$\frac{\Delta m_{21}^2}{10^{-9} eV^2}$	$7.42^{+0.21}_{-0.20}$	6.82 \rightarrow 8.04	$7.42^{+0.21}_{-0.20}$	6.82 \rightarrow 8.04
$\frac{\Delta m_{3l}^2}{10^{-3} eV^2}$	$+2.515^{+0.028}_{-0.028}$	+2.431 \rightarrow +2.599	$-2.498^{+0.028}_{-0.029}$	-2.584 \rightarrow -2.413

TABLE II: Neutrino oscillation parameters from NuFIT [47].

It should be noted that minimum χ^2 alone is not sufficient to determine the best mass model because it does not provide any information regarding the degree of fine tuning in the mass matrix elements that is needed to reproduce the experimental data. In order to clarify this issue, we will present a quantitative analysis regarding the degree of fine tuning in the elements of the neutrino mass matrix. In case of TM₁ and TM₂ mixing matrix, the elements of the neutrino mass matrix depend on two unknown parameters θ and ϕ . The dimensionless quantity d_{FT} which measures the amount of fine tuning in the neutrino mass matrix element is defined as the sum of the absolute values of the ratios between each parameter and its error [15, 48]. We define d_{FT} as

$$d_{FT} = \sum \left| \frac{par_i}{err_i} \right|, \quad (20)$$

where par_i is the best fit values of the parameters θ and ϕ , respectively. The error err_i for each parameter is calculated from the shift in the best fit value that changes χ_{min}^2 value by one unit while keeping other parameters fixed at their best fit values. Also we define d_{Data} as the ratio of sum of absolute values of each parameter and their error. Using the data from Table. II, we obtain d_{Data} to be around 100. The d_{FT} parameter can provide a rough estimate of the degree of fine tuning in the mass matrix elements because if the d_{FT} value is large then there will be large difference in the χ^2 for a small change in the corresponding parameter. Hence a large value of d_{FT} corresponds to a strong fine tuning of the mass matrix elements and vice versa.

We now proceed to analyse all the two minor zero classes one by one.

A. Class: A_1

Class A_1 corresponds to the minor zero for the (3, 3) and the (3, 2) elements of the neutrino mass matrix. The corresponding equations satisfying two minor zero conditions can be written as

$$\begin{aligned} (M)_{ee}(M)_{\mu\mu} - (M)_{e\mu}(M)_{\mu e} &= 0, \\ (M)_{ee}(M)_{\mu\tau} - (M)_{\mu e}(M)_{e\tau} &= 0. \end{aligned} \quad (21)$$

Using Eq. 16, the mass ratios for TM₁ can be expressed as

$$\begin{aligned} \frac{m_1}{m_2} e^{-2i\alpha} &= \frac{-\cos\theta}{2\sqrt{3}\left(\frac{1}{\sqrt{3}}\cos\theta + \frac{1}{\sqrt{2}}\sin\theta e^{-i\phi}\right)}, \\ \frac{m_1}{m_3} e^{-2i\beta} &= \frac{-\sin\theta}{2\sqrt{3}\left(\frac{1}{\sqrt{3}}\sin\theta - \frac{1}{\sqrt{2}}\cos\theta e^{-i\phi}\right)}, \\ \frac{m_3}{m_2} e^{-2i(\alpha+\beta)} &= \frac{\cos\theta\left(\frac{1}{\sqrt{3}}\sin\theta - \frac{1}{\sqrt{2}}\cos\theta e^{-i\phi}\right)}{\sin\theta\left(\frac{1}{\sqrt{3}}\cos\theta + \frac{1}{\sqrt{2}}\sin\theta e^{-i\phi}\right)}. \end{aligned} \quad (22)$$

Similarly, for TM_2 mixing matrix, the mass ratios can be expressed as

$$\begin{aligned}\frac{m_1}{m_2}e^{-2i\alpha} &= \frac{-(\cos\theta + \sqrt{3}\sin\theta e^{i\phi})}{2\cos\theta}, \\ \frac{m_1}{m_3}e^{-2i\beta} &= \frac{\sin\theta(\frac{1}{\sqrt{6}}\cos\theta + \frac{1}{\sqrt{2}}\sin\theta e^{i\phi})}{\cos\theta(\frac{1}{\sqrt{6}}\sin\theta - \frac{1}{\sqrt{2}}\cos\theta e^{i\phi})}, \\ \frac{m_3}{m_2}e^{-2i(\alpha+\beta)} &= \frac{-\sin\theta + \sqrt{3}\cos\theta e^{i\phi}}{2\sin\theta}.\end{aligned}\quad (23)$$

The χ_{min}^2 value and the d_{FT} parameter for Class A_1 are listed in Table. III. It is evident that the fine tuning parameter d_{FT} is quite large in case of TM_1 mixing matrix compared to TM_2 mixing matrix for this class. Hence the degree of fine tuning in the elements of neutrino mass matrix is quite strong in case of TM_1 mixing matrix. The corresponding best fit values of our model parameters θ and ϕ along with all the neutrino oscillation parameters namely, the three mixing angles (θ_{13} , θ_{23} , θ_{12}), two mass squared differences (Δm_{21}^2 , Δm_{32}^2), the Jarlskog invariant J and Dirac CP violating phase δ obtained for this class are reported in Table. III. It is evident from Eq. 6 and Eq. 7 that θ_{23} is invariant under the transformation $\phi \rightarrow (2\pi - \phi)$, hence we get two best fit values of ϕ . Similarly, we get two values of J and δ corresponding to two best fit values of ϕ . The best fit values of the mixing angles θ_{12} , θ_{13} and the mass squared differences Δm_{21}^2 , Δm_{32}^2 obtained for this class are compatible with the experimentally measured values reported in Table. II. It is observed that, in case of TM_2 mixing matrix, the best fit value of θ_{23} is compatible with the experimentally measured value but for TM_1 mixing matrix the best fit value deviates significantly from the experimentally measured value. Moreover, in case of TM_2 mixing matrix, the best fit value of θ_{12} deviates from the measured value of θ_{12} at more than 2σ significance.

Mixing matrix	χ_{min}^2	d_{FT}	ϕ°	θ°	θ_{12}°	θ_{13}°	θ_{23}°	J	δ°	$\Delta m_{21}^2 (10^{-5}eV^2)$	$\Delta m_{32}^2 (10^{-3}eV^2)$
TM_1	33.37	1.24×10^2	101.67, 258.32	14.67	34.37	8.41	42.62	$\pm 3.26 \times 10^{-2}$	79.32, 280.68	7.47	2.50
TM_2	20.61	1.25	37.59, 322.41	10.03	35.68	8.17	49.61	$\pm 2.01 \times 10^{-2}$	38.17, 321.83	7.55	2.48

TABLE III: χ_{min}^2 , d_{FT} , best fit values of ϕ° , θ° , θ_{12}° , θ_{13}° , θ_{23}° , J , δ° , $\Delta m_{21}^2 (10^{-5}eV^2)$ and $\Delta m_{32}^2 (10^{-3}eV^2)$ for TM_1 and TM_2 mixing matrix for Class A_1 .

For the TM_1 mixing matrix, we use Eq. 6 and vary θ_{13} within 3σ from the central value and obtain the 3σ allowed range of θ to be ($14.26^\circ - 15.64^\circ$). Using the allowed range of θ and imposing the additional constraint coming from r , we obtain the allowed ranges of θ_{12} and θ_{23} to be ($34.25^\circ - 34.42^\circ$) and ($40.01^\circ - 44.02^\circ$), respectively. It is clear that the value of θ_{23} obtained in this case lies in the lower octant, i.e, for the TM_1 mixing matrix, this pattern prefers the atmospheric mixing angle to be smaller than $\pi/4$. We show the variation of θ_{23} as a function of the unknown parameter ϕ in Fig. 1a. The corresponding best fit value of θ_{23} is shown with '*' mark in Fig. 1a. We show the variation of J and δ as a function of ϕ in Fig. 1b and Fig. 1c, respectively. It is observed that the Jarlskog rephasing invariant J and the Dirac CP violating phase δ are restricted to two regions. We obtain the 3σ allowed ranges of J and δ to be $[(-3.12 \times 10^{-2}, -3.43 \times 10^{-2}), (3.12 \times 10^{-2}, 3.43 \times 10^{-2})]$ and $[(68.66, 85.48)^\circ, (274.51, 291.33)^\circ]$, respectively.

For the TM_2 mixing matrix, we use Eq. 7 and obtain the 3σ allowed range of θ to be ($10.03^\circ - 10.99^\circ$). The corresponding allowed ranges of θ_{12} and θ_{23} are found to be ($35.68^\circ - 35.75^\circ$) and ($39.00^\circ - 50.99^\circ$), respectively. We show the variation of θ_{23} as a function of the unknown parameter ϕ in Fig. 2a. We also show the variation of J and δ as a function of ϕ in Fig. 2b and Fig. 2c, respectively. The 3σ allowed ranges of J and δ are found to be $[0, \pm 3.39 \times 10^{-2}]$ and $[(0, 90)^\circ, (270, 360)^\circ]$, respectively.

We show the variation of neutrino masses m_1 , m_2 and m_3 as a function of ϕ in Fig 3a and Fig. 4a for TM_1 and TM_2 mixing matrix, respectively. It shows normal mass ordering for both TM_1 and TM_2 mixing matrix. In Fig 3b and Fig. 4b, we show the variation of $\sum m_i$ as a function of ϕ . The correlation of M_{ee} and $\sum m_i$ for TM_1 and TM_2 mixing matrix are shown in Fig. 3c and Fig. 4c, respectively. In Fig. 3d and Fig. 4d, we have shown the correlation of m_ν with $\sum m_i$ for TM_1 and TM_2 mixing matrix, respectively. The variation of Majorana phases α and β as a function of ϕ is shown in Fig. 3e and Fig. 3f for TM_1 mixing matrix and in Fig. 4e and Fig. 4f for TM_2 mixing matrix, respectively.

The best fit values and the corresponding 3σ allowed ranges of the absolute neutrino mass scale, the effective Majorana neutrino mass, the effective electron anti-neutrino mass and CP violating phases α and β are listed in Table. IV. It is observed that the CP violating Majorana phases α and β are restricted to two regions. For TM_1 mixing matrix, the best fit values of α and β are obtained to be ± 9.28 and ± 33.48 , respectively. Similarly, for the TM_2 mixing matrix, the best fit values of α and β are found to be ± 6.62 and ± 16.46 , respectively. The upper bound

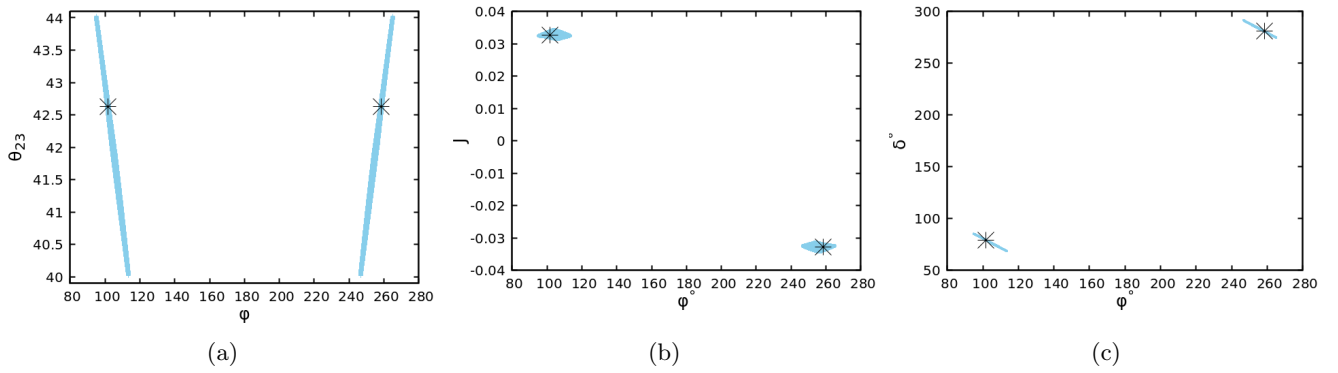


Figure 1: (a) Variation of θ_{23} as a function of ϕ , (b) variation of J as a function of ϕ , and (c) variation of δ as a function of ϕ for TM_1 mixing matrix for Class A_1 . The '*' mark in the figures represents the best fit value.

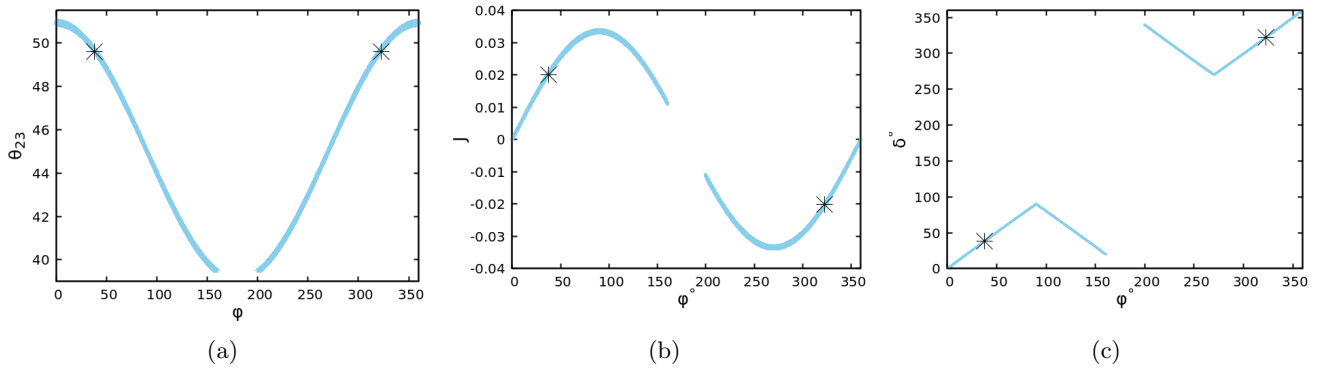


Figure 2: (a) Variation of θ_{23} as a function of ϕ , (b) variation of J as a function of ϕ , and (c) variation of δ as a function of ϕ for TM_2 mixing matrix for Class A_1 . The '*' mark in the figures represents the best fit value.

of M_{ee} obtained for this class is of $\mathcal{O}(10^{-2})$ and is within the sensitivity reach of neutrinoless double beta decay. The upper bound on the effective electron anti-neutrino mass $m_\nu < 0.012 \text{ eV}$ is beyond the reach of current β decay experiments.

Mixing matrix	Values	$\sum m_i$ (eV)	M_{ee} (eV)	m_ν (eV)	α°	β°
TM_1	Best fit	0.066	0.006	0.010	± 9.28	± 33.48
	3σ Range	[0.060, 0.073]	[0.001, 0.007]	[0.009, 0.011]	[(-10.03, -8.84), (8.84, 10.03)]	[(-36.79, -27.82), (27.82, 36.79)]
TM_2	Best fit	0.069	0.009	0.011	± 6.62	± 16.46
	3σ Range	[0.058, 0.071]	[0.005, 0.010]	[0.009, 0.012]	[0, ± 9.18]	[0, ± 44.99]

TABLE IV: Best fit and 3σ allowed range of $\sum m_i$ (eV), M_{ee} (eV), m_ν (eV), α° and β° for Class A_1 .

B. Class: A_2

For Class A_2 , the minors corresponding to the (2, 2) and (3, 2) elements of the neutrino mass matrix are zero. The minor zero conditions for this class can be written in terms of the neutrino mass matrix elements as

$$\begin{aligned}
 (M)_{ee}(M)_{\tau\tau} - (M)_{e\tau}(M)_{\tau e} &= 0, \\
 (M)_{ee}(M)_{\mu\tau} - (M)_{\mu e}(M)_{e\tau} &= 0.
 \end{aligned}
 \tag{24}$$

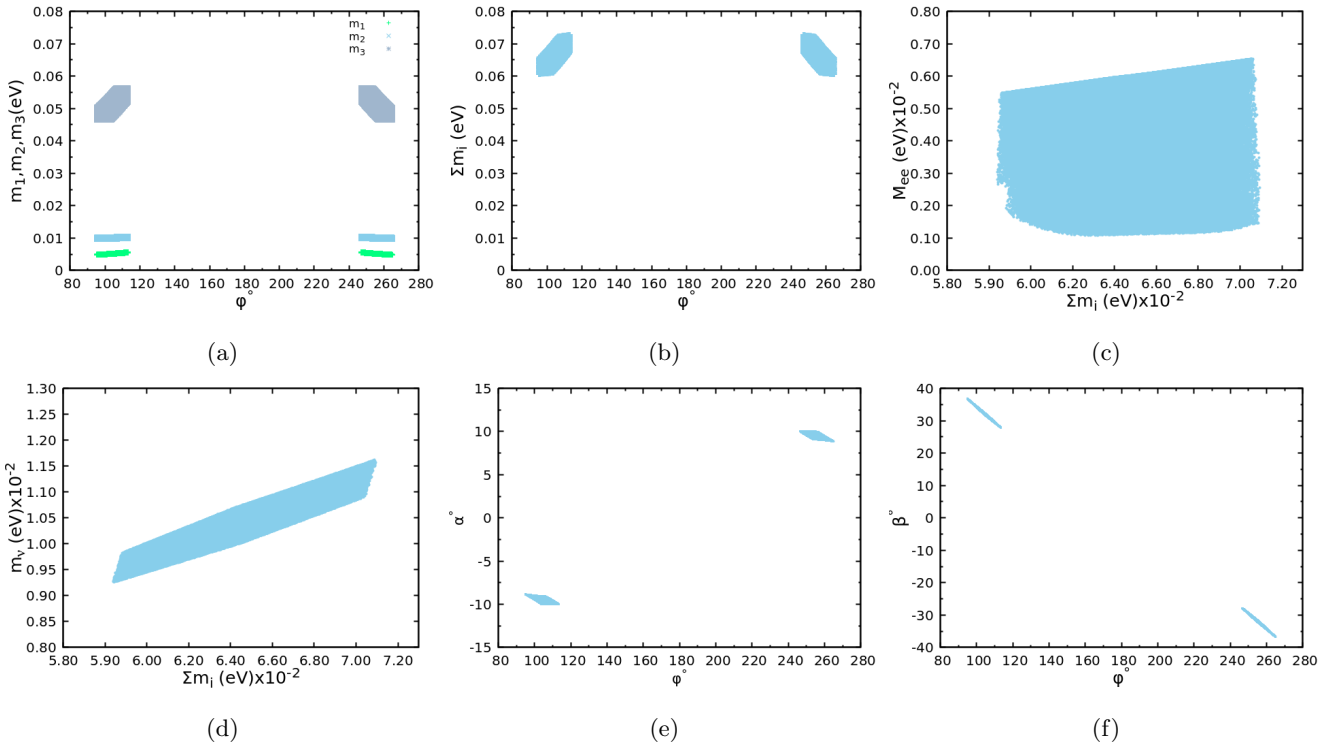


Figure 3: (a) Variation of m_1, m_2, m_3 as a function of ϕ , (b) variation of $\sum m_i$ as a function of ϕ , (c) correlation between $\sum m_i$ and M_{ee} , (d) correlation between $\sum m_i$ and m_ν , (e) variation of α as a function of ϕ , and (f) variation of β as a function of ϕ for TM_1 mixing matrix for Class A_1 .

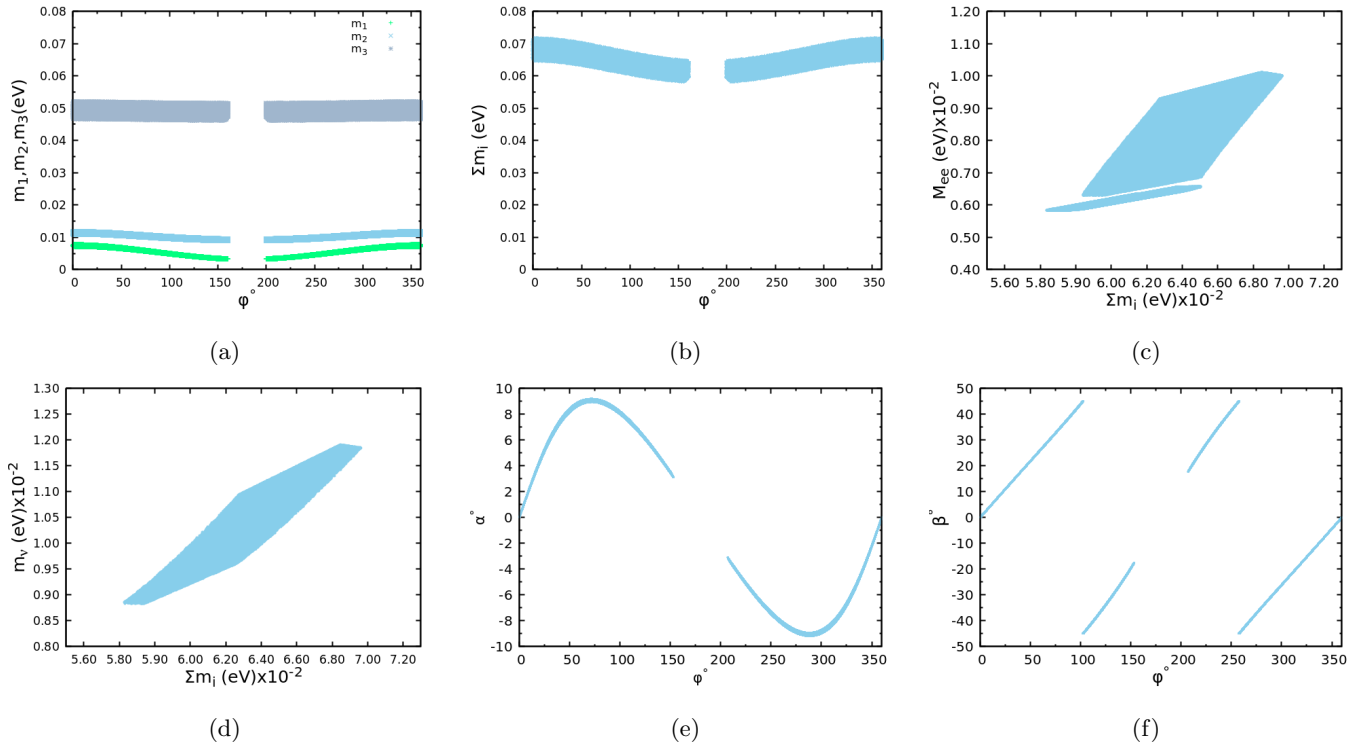


Figure 4: (a) Variation of m_1, m_2, m_3 as a function of ϕ , (b) variation of $\sum m_i$ as a function of ϕ , (c) correlation between $\sum m_i$ and M_{ee} , (d) correlation between $\sum m_i$ and m_ν , (e) variation of α as a function of ϕ , and (f) variation of β as a function of ϕ for TM_2 mixing matrix for Class A_1 .

The mass ratios for TM_1 and TM_2 mixing matrix can be expressed as

$$\begin{aligned}\frac{m_1}{m_2}e^{-2i\alpha} &= \frac{-\cos\theta}{2\sqrt{3}\left(\frac{1}{\sqrt{3}}\cos\theta - \frac{1}{\sqrt{2}}\sin\theta e^{-i\phi}\right)}, \\ \frac{m_1}{m_3}e^{-2i\beta} &= \frac{-\sin\theta}{2\sqrt{3}\left(\frac{1}{\sqrt{3}}\sin\theta + \frac{1}{\sqrt{2}}\cos\theta e^{-i\phi}\right)}, \\ \frac{m_3}{m_2}e^{-2i(\alpha+\beta)} &= \frac{\cos\theta\left(\frac{1}{\sqrt{3}}\sin\theta + \frac{1}{\sqrt{2}}\cos\theta e^{-i\phi}\right)}{\sin\theta\left(\frac{1}{\sqrt{3}}\cos\theta - \frac{1}{\sqrt{2}}\sin\theta e^{-i\phi}\right)}.\end{aligned}\quad (25)$$

and

$$\begin{aligned}\frac{m_1}{m_2}e^{-2i\alpha} &= \frac{-\cos\theta + \sqrt{3}\sin\theta e^{i\phi}}{2\cos\theta}, \\ \frac{m_1}{m_3}e^{-2i\beta} &= \frac{\sin\theta\left(\frac{1}{\sqrt{6}}\cos\theta - \frac{1}{\sqrt{2}}\sin\theta e^{i\phi}\right)}{\cos\theta\left(\frac{1}{\sqrt{6}}\sin\theta + \frac{1}{\sqrt{2}}\cos\theta e^{i\phi}\right)}, \\ \frac{m_3}{m_2}e^{-2i(\alpha+\beta)} &= \frac{-(\sin\theta + \sqrt{3}\cos\theta e^{i\phi})}{2\sin\theta}.\end{aligned}\quad (26)$$

We report the values of χ_{min}^2 and d_{FT} for Class A_2 in Table. V. The fine tuning parameter d_{FT} is found to be quite large in case of TM_1 mixing matrix. So, for this class, the degree of fine tuning of the elements of neutrino mass matrix is strong in case of TM_1 mixing matrix although χ_{min}^2 value obtained is quite small. Corresponding best fit values of our model parameters θ and ϕ along with all the neutrino oscillation parameters namely, the three mixing angles (θ_{13} , θ_{23} , θ_{12}), two mass squared differences (Δm_{21}^2 , Δm_{32}^2), the Jarlskog invariant J and Dirac CP violating phase δ obtained for this class are reported in Table. V. The best fit values of the mixing angles θ_{12} , θ_{13} , θ_{23} and the mass squared differences Δm_{21}^2 , Δm_{32}^2 obtained are compatible with the experimentally measured values. It should, however, be noted that the best fit value of θ_{12} for the TM_2 mixing matrix differs from the experimentally measured central value at more than 2σ significance. This is quite a generic feature of TM_2 mixing matrix.

Mixing matrix	χ_{min}^2	d_{FT}	ϕ°	θ°	θ_{12}°	θ_{13}°	θ_{23}°	J	δ°	$\Delta m_{21}^2 (10^{-5}\text{eV}^2)$	$\Delta m_{32}^2 (10^{-3}\text{eV}^2)$
TM_1	1.65	5.63×10^2	72.55, 287.45	15.02	34.33	8.60	48.60	$\pm 3.25 \times 10^{-2}$	74.07, 285.93	7.42	2.59
TM_2	23.28	1.30	46.68, 313.31	10.00	35.67	8.14	48.96	$\pm 2.39 \times 10^{-2}$	47.29, 312.71	7.62	2.47

TABLE V: χ_{min}^2 , d_{FT} , best fit values of ϕ° , θ° , θ_{12}° , θ_{13}° , θ_{23}° , J , δ° , $\Delta m_{21}^2 (10^{-5}\text{eV}^2)$ and $\Delta m_{32}^2 (10^{-3}\text{eV}^2)$ for Class A_2 .

For the TM_1 mixing matrix, the allowed range of θ , obtained by using the 3σ experimental range of θ_{13} reported in Table. II, is ($14.26^\circ - 15.64^\circ$). Using the allowed range of θ , we obtain the allowed ranges of θ_{12} and θ_{23} to be ($34.25^\circ - 34.42^\circ$) and ($45.97^\circ - 49.98^\circ$), respectively. We also use the constraint coming from r to constrain the allowed parameter space. It is clear that the value of θ_{23} obtained in this case lies in the upper octant, i.e, for the TM_1 mixing matrix, this pattern prefers the atmospheric mixing angle to be higher than $\pi/4$. We show the variation of J and δ as a function of ϕ in Fig. 5b and Fig. 5c, respectively. We obtain the 3σ allowed ranges of J and δ to be $[(-3.12 \times 10^{-2}, -3.43 \times 10^{-2}), (3.12 \times 10^{-2}, 3.43 \times 10^{-2})]$ and $[(68.66, 85.48)^\circ, (274.51, 291.33)^\circ]$, respectively. Similar to Class A_1 , it is observed that the Jarlskog rephasing invariant J and the Dirac CP violating phase δ are restricted to two regions.

For the TM_2 mixing matrix, the 3σ allowed range of θ is found to be ($10.03^\circ - 10.99^\circ$). Corresponding 3σ allowed range of θ_{12} and θ_{23} are ($35.68^\circ - 35.75^\circ$) and ($39.00^\circ - 50.99^\circ$), respectively. We show the variation of θ_{23} as a function of the unknown parameter ϕ in Fig. 6a. The 3σ allowed ranges of J and δ are found to be $[0, \pm 3.39 \times 10^{-2}]$ and $[(0, 90)^\circ, (270, 360)^\circ]$, respectively. We also show the variation of J and δ as a function of ϕ in Fig. 6b and Fig. 6c, respectively.

Let us now proceed to discuss the phenomenological implication of class A_2 pattern on neutrino masses, the effective Majorana mass, effective electron anti-neutrino mass and the CP violating Majorana phases. We show the variation of neutrino masses m_1 , m_2 and m_3 as a function of ϕ in Fig 7a and Fig. 8a for the TM_1 and the TM_2 mixing matrix, respectively. In each case, they show normal mass ordering. The variation of $\sum m_i$ as a function of ϕ is shown in Fig 7b and Fig. 8b for TM_1 and TM_2 mixing matrix, respectively. In Fig. 7c and Fig. 8c, we have shown the correlation of M_{ee} and $\sum m_i$ for both the mixing matrix, respectively. We have shown the correlation of m_ν with

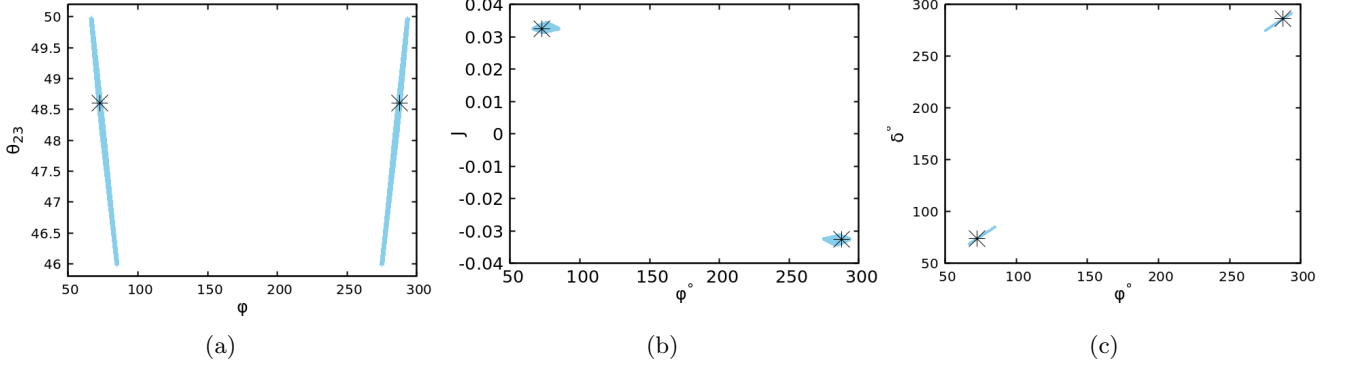


Figure 5: (a) Variation of θ_{23} as a function of ϕ , (b) variation of J as a function of ϕ , and (c) variation of δ as a function of ϕ for TM_1 mixing matrix for Class A_2 . The '*' mark in the figures represents the best fit value.

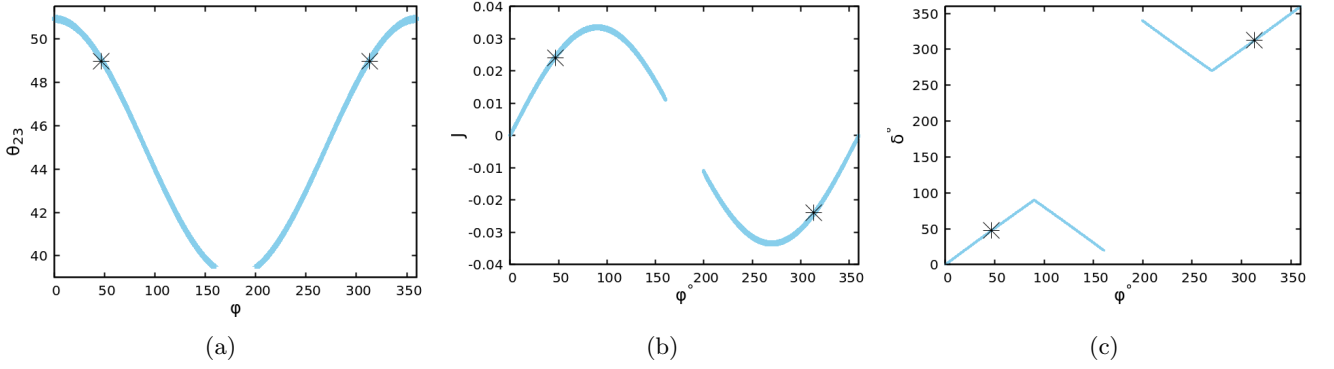


Figure 6: (a) Variation of θ_{23} as a function of ϕ , (b) variation of J as a function of ϕ , and (c) variation of δ as a function of ϕ for TM_2 mixing matrix for Class A_2 . The '*' mark in the figures represents the best fit value.

$\sum m_i$ for TM_1 and TM_2 mixing matrix in Fig. 7d and Fig. 8d, respectively. Also in Fig. 7e and Fig. 8e, we have shown the variation of α with respect to ϕ for both TM_1 and TM_2 mixing matrix, respectively. In Fig. 7f and Fig. 8f, we have shown the variation of β with respect to ϕ for both the mixing matrix. The phenomenology of this class is quite similar to class A_1 .

The best fit values and the corresponding allowed ranges of the absolute neutrino mass scale, the effective Majorana mass, the effective electron anti-neutrino mass and Majorana CP violating phases for this class are listed in Table. VI. The best fit values and the allowed ranges of each observables obtained for this class are quite similar to the values obtained for class A_1 .

Mixing matrix	Values	$\sum m_i$ (eV)	M_{ee} (eV)	m_ν (eV)	α°	β°
TM_1	Best fit	0.066	0.006	0.010	± 9.58	± 30.73
	3σ Range	[0.060, 0.073]	[0.006, 0.007]	[0.009, 0.012]	$[(-10.03, -8.84), (8.84, 10.03)]$	$[(-36.79, -27.82), (27.82, 36.79)]$
TM_2	Best fit	0.064	0.006	0.009	± 7.84	± 29.21
	3σ Range	[0.057, 0.071]	[0.006, 0.009]	[0.008, 0.012]	$[0, \pm 9.18]$	$[0, \pm 44.99]$

TABLE VI: Best fit and 3σ allowed range of $\sum m_i$ (eV), M_{ee} (eV), m_ν (eV), α° and β° for Class A_2 .

C. Other Classes

The classes $B_3, B_4, B_5, B_6, S_1, S_2, F_1, F_2$ and F_3 are not acceptable for both TM_1 and TM_2 mixing matrix because the value of r obtained for these classes are not within the experimental range. Similarly, the classes S_3, F_4 and F_5 are not allowed since they predict $m_1 = m_2$ for both TM_1 and TM_2 mixing matrix, respectively. Moreover, the class

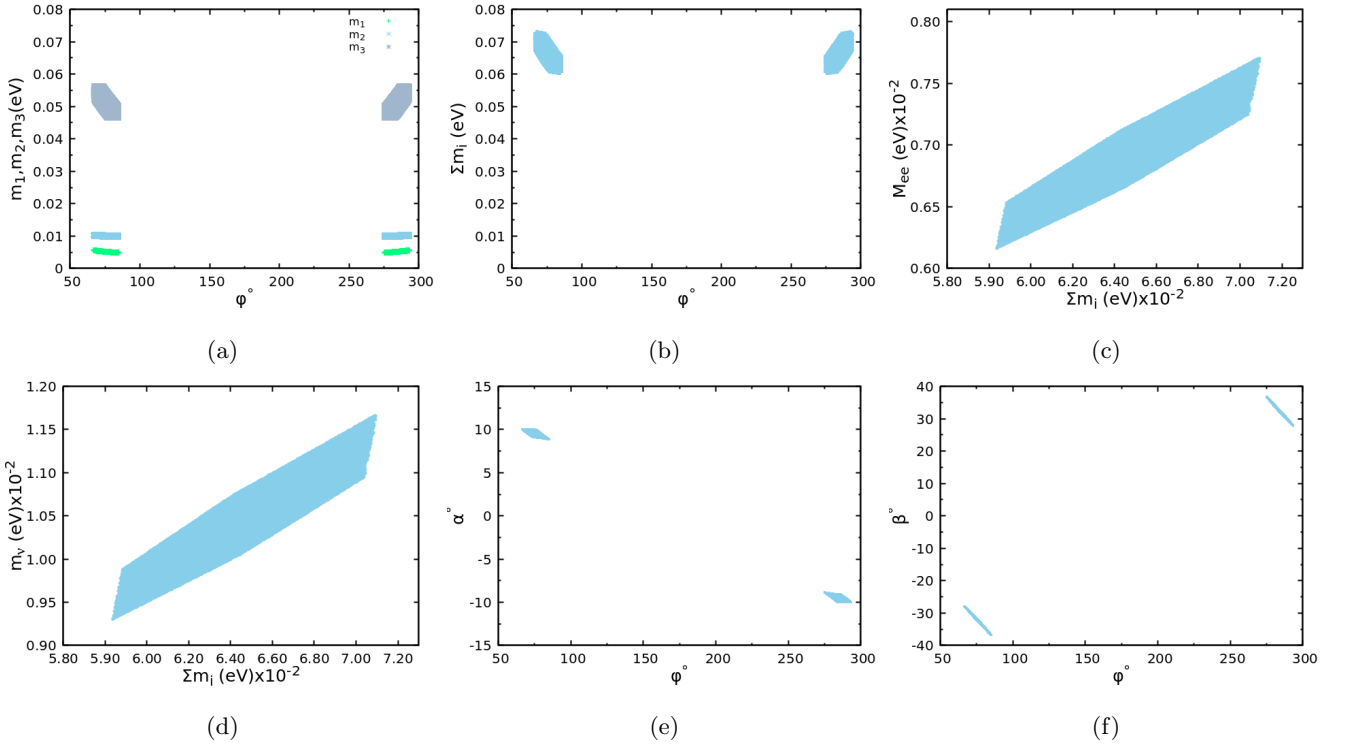


Figure 7: (a) Variation of m_1, m_2, m_3 as a function of ϕ , (b) variation of $\sum m_i$ as a function of ϕ , (c) correlation between $\sum m_i$ and M_{ee} , (d) correlation between $\sum m_i$ and m_ν , (e) variation of α as a function of ϕ , and (f) variation of β as a function of ϕ for TM_1 mixing matrix for Class A_2 .

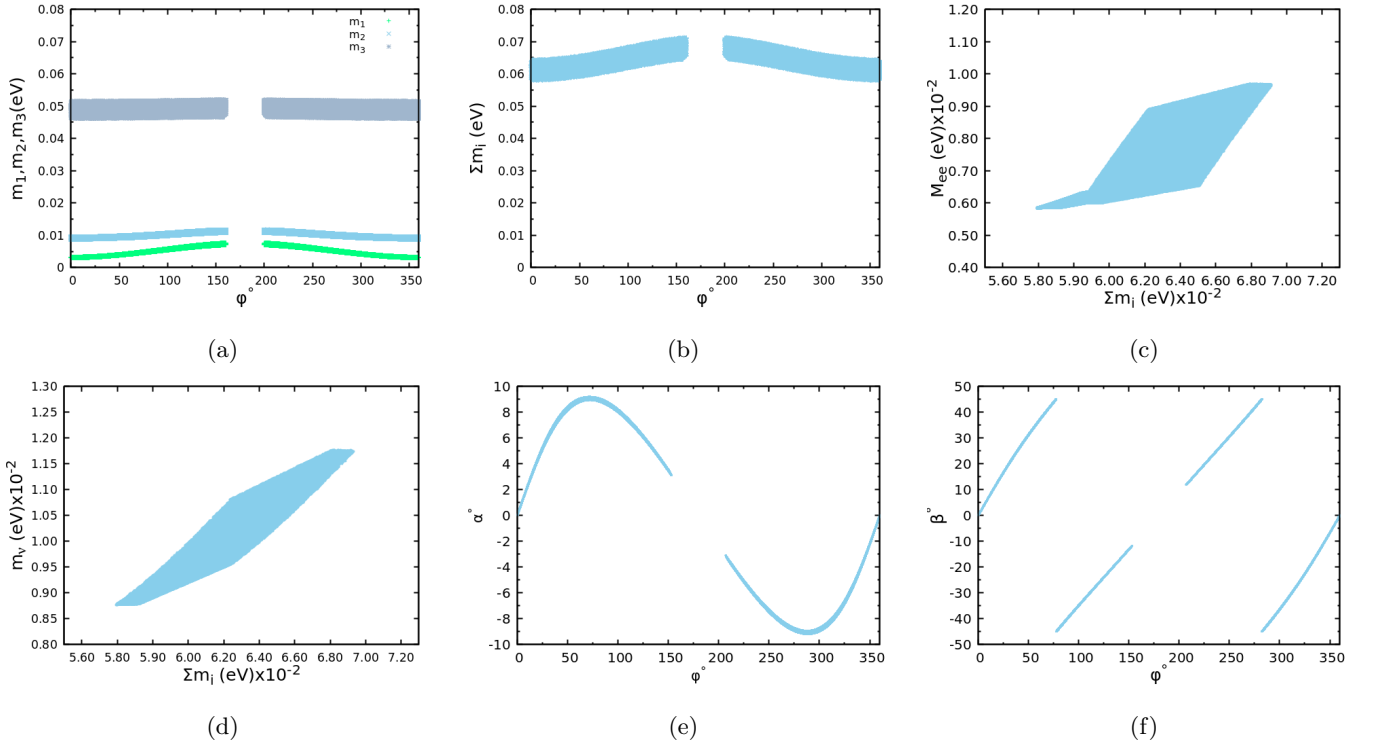


Figure 8: (a) Variation of m_1, m_2, m_3 as a function of ϕ , (b) variation of $\sum m_i$ as a function of ϕ , (c) correlation between $\sum m_i$ and M_{ee} , (d) correlation between $\sum m_i$ and m_ν , (e) variation of α as a function of ϕ , and (f) variation of β as a function of ϕ for TM_2 mixing matrix for Class A_2 .

D is also not allowed as this class predicts $m_3 = m_2$ for TM_1 mixing matrix and $m_1 = m_3$ for TM_2 mixing matrix, respectively.

V. SYMMETRY REALIZATION

We can realize the symmetry of two minor zero in neutrino mass matrix through type-I seesaw mechanism along with Abelian symmetry. For generating leptonic mass matrix, we need three right handed neutrinos ν_{Rp} ($p = 1, 2, 3$), three right handed charged leptons l_{Rp} and three left handed lepton doublets D_{Lp} . Along with these, we need Higgs doublet for non zero elements $(M_l)_{pq}$ or $(M_D)_{pq}$, and scalar singlet for non zero elements $(M_R)_{pq}$ where $q = 1, 2, 3$. Higgs doublets get vacuum expectation values (vevs) at the electroweak scale and the scalar singlets get the vevs at the seesaw scale. We follow the procedure discussed in Refs. [10, 20] to present the symmetry realization of class A_1 using Z_8 symmetry group. Under Z_8 symmetry, the leptons of first family remain invariant, leptons of second family changes sign and leptons of third family get multiplied by $\omega = \exp(\frac{i\pi}{4})$.

The leptonic fields under Z_8 transform as

$$\begin{aligned} \bar{l}_{R1} &\rightarrow \bar{l}_{R1}, & \bar{\nu}_{R1} &\rightarrow \bar{\nu}_{R1}, & D_{L1} &\rightarrow \bar{D}_{L1}, \\ \bar{l}_{R2} &\rightarrow \omega^4 \bar{l}_{R2}, & \bar{\nu}_{R2} &\rightarrow \omega^4 \bar{\nu}_{R2}, & D_{L2} &\rightarrow \omega^4 \bar{D}_{L2}, \\ \bar{l}_{R3} &\rightarrow \omega \bar{l}_{R3}, & \bar{\nu}_{R3} &\rightarrow \omega \bar{\nu}_{R3}, & D_{L3} &\rightarrow \omega^7 \bar{D}_{L3}, \end{aligned} \quad (27)$$

The bilinears $\bar{l}_{Rp} D_{Lq}$ and $\bar{\nu}_{Rp} D_{Lq}$ relevant for $(M_l)_{pq}$ and $(M_D)_{pq}$ transform as

$$\bar{l}_{Rp} D_{Lq} \cong \bar{\nu}_{Rp} D_{Lq} \cong \begin{pmatrix} 1 & \omega^4 & \omega^7 \\ \omega^4 & 1 & \omega^3 \\ \omega & \omega^5 & 1 \end{pmatrix} \quad (28)$$

and the bilinears $\bar{\nu}_{Rp} \bar{\nu}_{Rq}$ relevant for $(M_R)_{pq}$ transform as

$$\bar{\nu}_{Rp} \bar{\nu}_{Rq} \cong \begin{pmatrix} 1 & \omega^4 & \omega \\ \omega^4 & 1 & \omega^5 \\ \omega & \omega^5 & \omega^2 \end{pmatrix}. \quad (29)$$

Under these transformation the diagonal Dirac mass matrices are generated automatically for both charged leptons and neutrinos. Also, under Z_8 transformation the elements (1, 1) and (2, 2) of Majorana mass matrix M_R remain invariant. We can obtain non zero elements (1, 2) by introducing real scalar field χ_{12} which changes sign under Z_8 transformation and (1, 3) by introducing complex scalar fields χ_{13} which under Z_8 transformation gets multiplied by ω^7 for M_R . In the absence of any scalar singlets other elements of M_R remain zero. The Majorana mass matrix M_R can be written as

$$M_R = \begin{pmatrix} 1 & b & c \\ b & 1 & 0 \\ c & 0 & 0 \end{pmatrix}. \quad (30)$$

This gives two minor zero conditions corresponding to Class A_1 in the neutrino mass matrix. Class A_2 can also be realised similarly for different M_R .

VI. CONCLUSION

We explore the consequences of two minor zeros in the neutrino mass matrix using trimaximal mixing matrix. There are total fifteen possible patterns and out of these only two patterns namely class A_1 and class A_2 are found to be phenomenologically acceptable for TM_1 and TM_2 mixing matrix, respectively. We perform a naive χ^2 analysis to find the best fit values of the two unknown parameters θ and ϕ of the TM mixing matrix. We include five observables in our χ^2 analysis namely, the three mixing angles ($\theta_{13}, \theta_{12}, \theta_{23}$) and the two mass squared differences ($\Delta m_{21}^2, \Delta m_{32}^2$). It is found that class A_2 with TM_1 mixing matrix provides the best fit to the experimental results. We also discuss the degree of fine tuning in the elements of the mass matrix for both classes A_1 and A_2 by introducing a new parameter d_{FT} . The d_{FT} value is quite large in case of TM_1 mixing matrix for both the classes although the χ_{min}^2 value obtained for Class A_2 is quite small. Based on the d_{FT} value, one can conclude that the degree of fine tuning in the mass matrix element is quite strong in case of TM_1 mixing matrix. The two allowed classes show normal mass ordering. We

also give prediction of several unknown parameters such as the absolute neutrino mass scale, the effective Majorana mass, the effective electron anti-neutrino mass, three CP violating phases and the Jarlskog invariant measure of CP violation. The effective Majorana mass obtained for each pattern is within the reach of neutrinoless double beta decay experiment. The upper bound on the effective electron anti-neutrino mass obtained for each pattern is beyond the reach of current β decay experiments. Moreover, we also discuss the symmetry realization of Class A_1 in the framework of type-I seesaw model using Abelian symmetry group Z_8 .

Appendix A

The elements of neutrino mass matrix using TM_1 mixing matrix can be written as

$$\begin{aligned}
(M)_{ee} &= \frac{2}{3} m_1 + \frac{1}{3} \cos^2 \theta m_2 e^{2i\alpha} + \frac{1}{3} \sin^2 \theta m_3 e^{2i\beta}, \\
(M)_{e\mu} &= \left(-\frac{1}{3}\right) m_1 + \left(\frac{1}{3} \cos^2 \theta - \frac{1}{\sqrt{6}} \sin \theta \cos \theta e^{i\phi}\right) m_2 e^{2i\alpha} + \left(\frac{1}{3} \sin^2 \theta + \frac{1}{\sqrt{6}} \sin \theta \cos \theta e^{i\phi}\right) m_3 e^{2i\beta}, \\
(M)_{e\tau} &= \left(-\frac{1}{3}\right) m_1 + \left(\frac{1}{3} \cos^2 \theta + \frac{1}{\sqrt{6}} \sin \theta \cos \theta e^{i\phi}\right) m_2 e^{2i\alpha} + \left(\frac{1}{3} \sin^2 \theta - \frac{1}{\sqrt{6}} \sin \theta \cos \theta e^{i\phi}\right) m_3 e^{2i\beta}, \\
(M)_{\mu\mu} &= \frac{1}{6} m_1 + \left(\frac{1}{\sqrt{3}} \cos \theta - \frac{1}{\sqrt{2}} \sin \theta e^{i\phi}\right)^2 m_2 e^{2i\alpha} + \left(\frac{1}{\sqrt{3}} \sin \theta + \frac{1}{\sqrt{2}} \cos \theta e^{i\phi}\right)^2 m_3 e^{2i\beta}, \\
(M)_{\mu\tau} &= \frac{1}{6} m_1 + \left(\frac{1}{3} \cos^2 \theta - \frac{1}{2} \sin^2 \theta e^{2i\phi}\right) m_2 e^{2i\alpha} + \left(\frac{1}{3} \sin^2 \theta - \frac{1}{2} \cos^2 \theta e^{2i\phi}\right) m_3 e^{2i\beta}, \\
(M)_{\tau\tau} &= \frac{1}{6} m_1 + \left(\frac{1}{\sqrt{3}} \cos \theta + \frac{1}{\sqrt{2}} \sin \theta e^{i\phi}\right)^2 m_2 e^{2i\alpha} + \left(\frac{1}{\sqrt{3}} \sin \theta - \frac{1}{\sqrt{2}} \cos \theta e^{i\phi}\right)^2 m_3 e^{2i\beta}.
\end{aligned} \tag{A1}$$

Using TM_2 mixing matrix, we can write the elements of neutrino mass matrix as

$$\begin{aligned}
(M)_{ee} &= \left(\frac{2}{3} \cos^2 \theta\right) m_1 + \frac{1}{3} m_2 e^{2i\alpha} + \left(\frac{2}{3} \sin^2 \theta\right) m_3 e^{2i\beta}, \\
(M)_{e\mu} &= \left(-\frac{1}{3} \cos^2 \theta + \frac{1}{\sqrt{3}} \sin \theta \cos \theta e^{-i\phi}\right) m_1 + \frac{1}{3} m_2 e^{2i\alpha} + \left(-\frac{1}{3} \sin^2 \theta - \frac{1}{\sqrt{3}} \sin \theta \cos \theta e^{-i\phi}\right) m_3 e^{2i\beta}, \\
(M)_{e\tau} &= \left(-\frac{1}{3} \cos^2 \theta - \frac{1}{\sqrt{3}} \sin \theta \cos \theta e^{-i\phi}\right) m_1 + \frac{1}{3} m_2 e^{2i\alpha} + \left(-\frac{1}{3} \sin^2 \theta + \frac{1}{\sqrt{3}} \sin \theta \cos \theta e^{-i\phi}\right) m_3 e^{2i\beta}, \\
(M)_{\mu\mu} &= \left(-\frac{1}{\sqrt{6}} \cos \theta + \frac{1}{\sqrt{2}} \sin \theta e^{-i\phi}\right)^2 m_1 + \frac{1}{3} m_2 e^{2i\alpha} + \left(\frac{1}{\sqrt{6}} \sin \theta + \frac{1}{\sqrt{2}} \cos \theta e^{-i\phi}\right)^2 m_3 e^{2i\beta}, \\
(M)_{\mu\tau} &= \left(\frac{1}{6} \cos^2 \theta - \frac{1}{2} \sin^2 \theta e^{-2i\phi}\right) m_1 + \frac{1}{3} m_2 e^{2i\alpha} + \left(\frac{1}{6} \sin^2 \theta - \frac{1}{2} \cos^2 \theta e^{-2i\phi}\right) m_3 e^{2i\beta}, \\
(M)_{\tau\tau} &= \left(\frac{1}{\sqrt{6}} \cos \theta + \frac{1}{\sqrt{2}} \sin \theta e^{-i\phi}\right)^2 m_1 + \frac{1}{3} m_2 e^{2i\alpha} + \left(-\frac{1}{\sqrt{6}} \sin \theta + \frac{1}{\sqrt{2}} \cos \theta e^{-i\phi}\right)^2 m_3 e^{2i\beta}.
\end{aligned} \tag{A2}$$

-
- [1] Y. Fukuda *et al.* [Super-Kamiokande], Phys. Rev. Lett. **81**, 1562-1567 (1998) doi:10.1103/PhysRevLett.81.1562 [arXiv:hep-ex/9807003 [hep-ex]].
- [2] G. L. Fogli, E. Lisi, D. Montanino and A. Palazzo, Phys. Rev. D **64**, 093007 (2001) doi:10.1103/PhysRevD.64.093007 [arXiv:hep-ph/0106247 [hep-ph]].
- [3] P. Minkowski, Phys. Lett. B **67**, 421-428 (1977) doi:10.1016/0370-2693(77)90435-X.
- [4] R. N. Mohapatra and G. Senjanovic, Phys. Rev. Lett. **44**, 912 (1980) doi:10.1103/PhysRevLett.44.912.
- [5] E. I. Lashin and N. Chamoun, Phys. Rev. D **80**, 093004 (2009) doi:10.1103/PhysRevD.80.093004 [arXiv:0909.2669 [hep-ph]].

- [6] I. A. Mazumder and R. Dutta, Phys. Rev. D **107**, no.11, 115023 (2023) doi:10.1103/PhysRevD.107.115023 [arXiv:2212.12884 [hep-ph]].
- [7] P. H. Frampton, S. L. Glashow and D. Marfatia, Phys. Lett. B **536**, 79-82 (2002) doi:10.1016/S0370-2693(02)01817-8 [arXiv:hep-ph/0201008 [hep-ph]].
- [8] S. Kumar and R. R. Gautam, Phys. Rev. D **96**, no.1, 015020 (2017) doi:10.1103/PhysRevD.96.015020 [arXiv:1706.03258 [hep-ph]].
- [9] Z. z. Xing, Phys. Lett. B **539**, 85-90 (2002) doi:10.1016/S0370-2693(02)02062-2 [arXiv:hep-ph/0205032 [hep-ph]].
- [10] L. Lavoura, Phys. Lett. B **609**, 317-322 (2005) doi:10.1016/j.physletb.2005.01.047 [arXiv:hep-ph/0411232 [hep-ph]].
- [11] S. Dev, S. Kumar, S. Verma and S. Gupta, Phys. Rev. D **76**, 013002 (2007) doi:10.1103/PhysRevD.76.013002 [arXiv:hep-ph/0612102 [hep-ph]].
- [12] S. Kumar, Phys. Rev. D **84**, 077301 (2011) doi:10.1103/PhysRevD.84.077301 [arXiv:1108.2137 [hep-ph]].
- [13] H. Fritzsch, Z. z. Xing and S. Zhou, JHEP **09**, 083 (2011) doi:10.1007/JHEP09(2011)083 [arXiv:1108.4534 [hep-ph]].
- [14] P. O. Ludl, S. Morisi and E. Peinado, Nucl. Phys. B **857**, 411-423 (2012) doi:10.1016/j.nuclphysb.2011.12.017 [arXiv:1109.3393 [hep-ph]].
- [15] D. Meloni and G. Blankenburg, Nucl. Phys. B **867**, 749-762 (2013) doi:10.1016/j.nuclphysb.2012.10.011 [arXiv:1204.2706 [hep-ph]].
- [16] W. Grimus and P. O. Ludl, J. Phys. G **40**, 055003 (2013) doi:10.1088/0954-3899/40/5/055003 [arXiv:1208.4515 [hep-ph]]. Dev:2015lya
- [17] R. R. Gautam and S. Kumar, Phys. Rev. D **94**, no.3, 036004 (2016) [erratum: Phys. Rev. D **100**, no.3, 039902 (2019)] doi:10.1103/PhysRevD.94.036004 [arXiv:1607.08328 [hep-ph]].
- [18] K. S. Channey and S. Kumar, J. Phys. G **46**, no.1, 015001 (2019) doi:10.1088/1361-6471/aaf55e [arXiv:1812.10268 [hep-ph]].
- [19] M. Singh, EPL **129**, no.1, 1 (2020) doi:10.1209/0295-5075/129/11002 [arXiv:1909.01552 [hep-ph]].
- [20] E. I. Lashin and N. Chamoun, Phys. Rev. D **85**, 113011 (2012) doi:10.1103/PhysRevD.85.113011 [arXiv:1108.4010 [hep-ph]].
- [21] R. R. Gautam, Phys. Rev. D **97**, no.5, 055022 (2018) doi:10.1103/PhysRevD.97.055022 [arXiv:1802.00425 [hep-ph]].
- [22] E. I. Lashin and N. Chamoun, Phys. Rev. D **78**, 073002 (2008) doi:10.1103/PhysRevD.78.073002 [arXiv:0708.2423 [hep-ph]].
- [23] S. Dev, S. Verma, S. Gupta and R. R. Gautam, Phys. Rev. D **81**, 053010 (2010) doi:10.1103/PhysRevD.81.053010 [arXiv:1003.1006 [hep-ph]].
- [24] S. Dev, S. Gupta and R. R. Gautam, Mod. Phys. Lett. A **26**, 501-514 (2011) doi:10.1142/S0217732311034906 [arXiv:1011.5587 [hep-ph]].
- [25] T. Araki, J. Heeck and J. Kubo, JHEP **07**, 083 (2012) doi:10.1007/JHEP07(2012)083 [arXiv:1203.4951 [hep-ph]].
- [26] J. Liao, D. Marfatia and K. Whisnant, JHEP **09**, 013 (2014) doi:10.1007/JHEP09(2014)013 [arXiv:1311.2639 [hep-ph]].
- [27] S. Dev, R. R. Gautam and L. Singh, Phys. Rev. D **87**, 073011 (2013) doi:10.1103/PhysRevD.87.073011 [arXiv:1303.3092 [hep-ph]].
- [28] W. Wang, Eur. Phys. J. C **73**, 2551 (2013) doi:10.1140/epjc/s10052-013-2551-2 [arXiv:1306.3556 [hep-ph]].
- [29] K. Whisnant, J. Liao and D. Marfatia, AIP Conf. Proc. **1604**, no.1, 273-278 (2015) doi:10.1063/1.4883441
- [30] S. Dev, L. Singh and D. Raj, Eur. Phys. J. C **75**, no.8, 394 (2015) doi:10.1140/epjc/s10052-015-3569-4 [arXiv:1506.04951 [hep-ph]].
- [31] W. Wang, S. Y. Guo and Z. G. Wang, Mod. Phys. Lett. A **31**, no.13, 1650080 (2016) doi:10.1142/S0217732316500802
- [32] K. Abe *et al.* [T2K], Phys. Rev. Lett. **107**, 041801 (2011) doi:10.1103/PhysRevLett.107.041801 [arXiv:1106.2822 [hep-ex]].

- [33] P. Adamson *et al.* [MINOS], Phys. Rev. Lett. **107**, 181802 (2011) doi:10.1103/PhysRevLett.107.181802 [arXiv:1108.0015 [hep-ex]].
- [34] Y. Abe *et al.* [Double Chooz], Phys. Rev. Lett. **108**, 131801 (2012) doi:10.1103/PhysRevLett.108.131801 [arXiv:1112.6353 [hep-ex]].
- [35] F. P. An *et al.* [Daya Bay], Phys. Rev. Lett. **108**, 171803 (2012) doi:10.1103/PhysRevLett.108.171803 [arXiv:1203.1669 [hep-ex]].
- [36] S. Kumar, Phys. Rev. D **82**, 013010 (2010) [erratum: Phys. Rev. D **85**, 079904 (2012)] doi:10.1103/PhysRevD.82.013010 [arXiv:1007.0808 [hep-ph]].
- [37] X. G. He and A. Zee, Phys. Rev. D **84**, 053004 (2011) doi:10.1103/PhysRevD.84.053004 [arXiv:1106.4359 [hep-ph]].
- [38] W. Grimus and L. Lavoura, JHEP **09**, 106 (2008) doi:10.1088/1126-6708/2008/09/106 [arXiv:0809.0226 [hep-ph]].
- [39] C. Jarlskog, Phys. Rev. Lett. **55**, 1039 (1985) doi:10.1103/PhysRevLett.55.1039
- [40] M. Aker *et al.* [KATRIN], Nature Phys. **18**, no.2, 160-166 (2022) doi:10.1038/s41567-021-01463-1 [arXiv:2105.08533 [hep-ex]].
- [41] A. A. Esfahani *et al.* [Project 8],[arXiv:2203.07349 [nucl-ex]].
- [42] M. Agostini *et al.* [GERDA], Phys. Rev. Lett. **111**, no.12, 122503 (2013) doi:10.1103/PhysRevLett.111.122503 [arXiv:1307.4720 [nucl-ex]].
- [43] A. Gando *et al.* [KamLAND-Zen], Phys. Rev. Lett. **110**, no.6, 062502 (2013) doi:10.1103/PhysRevLett.110.062502 [arXiv:1211.3863 [hep-ex]].
- [44] G. Anton *et al.* [EXO-200], Phys. Rev. Lett. **123**, no.16, 161802 (2019) doi:10.1103/PhysRevLett.123.161802 [arXiv:1906.02723 [hep-ex]].
- [45] M. Zhang, J. F. Zhang and X. Zhang, Commun. Theor. Phys. **72**, no.12, 125402 (2020) [arXiv:2005.04647 [astro-ph.CO]].
- [46] N. Palanque-Delabrouille, C. Yèche, N. Schöneberg, J. Lesgourgues, M. Walther, S. Chabanier and E. Armengaud, JCAP **04**, 038 (2020) doi:10.1088/1475-7516/2020/04/038 [arXiv:1911.09073 [astro-ph.CO]].
- [47] I. Esteban, M. C. Gonzalez-Garcia, M. Maltoni, T. Schwetz and A. Zhou, JHEP **09**, 178 (2020) doi:10.1007/JHEP09(2020)178 [arXiv:2007.14792 [hep-ph]].NuFIT 5.0(2020), <http://www.nu-fit.org>.
- [48] G. Altarelli and G. Blankenburg, JHEP **03**, 133 (2011) doi:10.1007/JHEP03(2011)133 [arXiv:1012.2697 [hep-ph]].